CONTROL OF INDUCTION MACHINE DRIVES IN OVERMODULATION RANGE

Van Tan Luong*, Doan Xuan Nam, Le Thanh Toi
Ho Chi Minh City University of Food Industry
*Email: *luongvt@hufi.edu.vn*
Received: 17 March 2020; Accepted: 8 May 2020

ABSTRACT

In this paper, a control scheme of a vector-controlled induction machine (IM) drives in overmodulation (OVM) range to maximize the voltage utilization of the voltage-source inverter (VSI) has been introduced. In OVM region, a modified voltage reference is produced for the space-vector pulse-width modulation (SVPWM), which can cause the motor current to be distorted, leading to the damage of the VSI control operation. To improve the system control performance, the harmonic current components in the feedback currents needs to be removed before feeding to the proportional-integral (PI) current controllers. The response of the current controllers in OVM range has been analyzed, which gives good performance of the system. The proposed method has been verified by simulation results for 3kW induction motor drives.

Keywords: Induction machine, overmodulation, vector control.

1. INTRODUCTION

A voltage-source inverter with a front-end diode rectifier, as illustrated in Figure 1 is commonly used in variable-speed machine drive applications. For these applications, a DC-link voltage is usually fixed and then the pulse-width modulation (PWM) voltage-source inverter (VSI) supplies the full voltage utilization of the inverters in overmodulation (OVM) techniques by modifying the voltage reference for the space vector pulse-width modulation (SVPWM).

Overmodulation refers to the operation of the pulse-width modulator beyond the linear range. In space-vector modulation, the maximum modulation index of 0.906 is achieved. However, the maximum possible voltage occurs during the six-step operation and is equal to $(2/\pi)V_{dc}$, which is known as modulation index. The region between the modulation indexes and is called overmodulation. Several OVM schemes have been presented for the SVPWM inverters extended up to the six-step mode operation [1-3].

A vector control of AC machines is usually used for fast torque control over a wide operating range. It can be applied for low and high power machine drive systems. A fast current control is required for the vector control to obtain decoupling and torque control. The current controllers force the measured machine current to follow the reference value and the output of these controllers produce the voltage reference for the modulation of the inverter. Normally, current regulators based on the proportional-integral (PI) control have been applied just for operating the DC quantity. To utilize fully the input voltage of the inverter, the pulse-width modulator must work in OVM range. Thus, adding lower order harmonics to the reference voltage causes distorted motor current, but it also achieves higher modulated output voltage [4]. The influence of these harmonics on the PI-type linear current controller is still a critical problem.

To tackle these issues, a method which compensates the harmonic components in the feedback current is proposed, where the first-order model is employed to estimate the harmonic components [4]. However, the method depends on the machine parameters for estimating the harmonic currents. Another method based on the sensorless control has been suggested for controlling induction motor drive [5]. Other researches have been introduced for the vector controlled machine drives in OVM range [6-8], where the SVPWM-based stator flux is employed. With this method, the voltage limitation of the inverter for SVPWM operation can be avoided. However, the machine parameters are required to accurately estimate the machine flux.

In this paper, a band-pass filter (BSF) is employed to remove the harmonic components in the feedback currents for the PI current controllers, which can improve the performance of the system in OVM range. The simulation results for 3kW induction motor drives in OVM range have been verified to the validity of the proposed method.

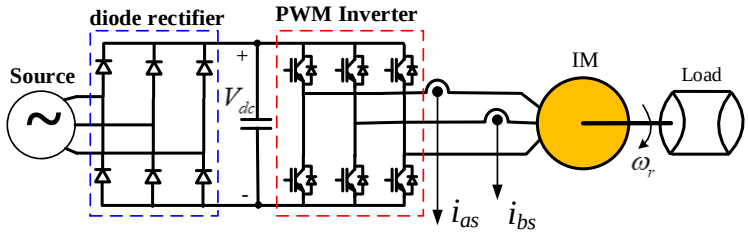

Figure 1. Induction machine drive system.

2. OVERMODULATION IN SPACE MODULATION

In the SVPWM, the three-phase voltage reference is provided as a voltage reference vector V^*. The maximum modulation index indicates the maximum value of modulated output of a pulse-width modulated inverter. The modulation index (m) is defined as the ratio of the peak value of the fundamental of the modulated output voltage to the peak value of the fundamental during six-step mode operation and is given by [9]

$$m = \frac{V^*}{(2/\pi)V_{dc}} \qquad (1)$$

where V^* and V_{dc} are the magnitude of the phase voltage reference and the inverter input voltage, respectively.

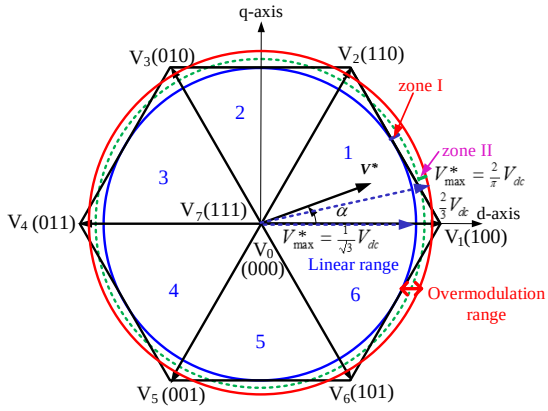

Figure 2. Diagram of voltage vectors in different operating modes.

OVM range is referred as the operation regions of the pulse-width modulator beyond the linear range (0.906) which is the inscribed circle of the hexagon. According to the modulation index, the PWM range is divided into three regions as seen in Figure 2. The voltage reference vector, its phase angle, and switching times for these vectors are described in detail [1].

2.1. Linear modulation ($0 \le m < 0.906$)

If the modulation index is lower or equal to 0.906, the space-vector modulator generates the sinusoidal output voltage. The space voltage vectors involve the six effective vectors and the two zero vectors, as shown in Figure 2. If the voltage reference vectors (V^*) is located in sector *1*, the effective vectors V_1, V_2 and the zero vector V_0 are employed to decide the durations of the switching pulse.

2.2. Overmodulation mode I ($0.906 < m \le 0.952$)

In zone I (mode I) of the OVM range, a trajectory of reference voltage vectors is partly outside of the hexagon. The compensated voltage magnitude is boosted to generate the desired fundamental voltage reference since it can not be produced by the PWM inverter. From the reference voltage vector (see Figure 2), the modified voltage reference vector in Figure 3 is derived by changing the magnitude of the reference voltage vector and keeping the phase angle at its original value.

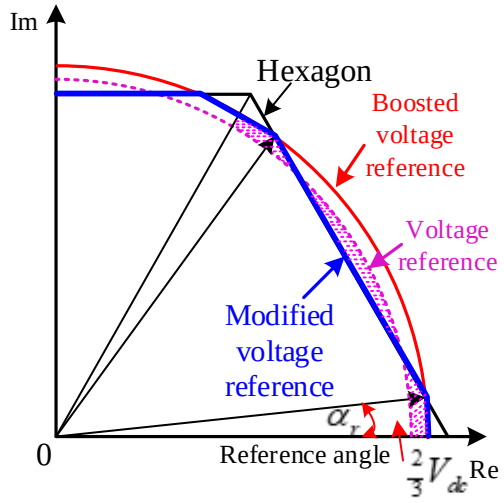

Figure 3. Voltage reference trajectory in overmodulation mode I (zone I).

2.3. Overmodulation mode II ($0.952 < m \le 1$)

As shown in Figure 4, in order to increase the modulation index further, actual voltage reference is kept at the vertex of the hexagon and the change in the angle of the modified reference vector is needed. Thus, the angular velocity is not changed continuously. When the modulation index reaches to value of 1, the modulator can operates under the six-step mode.

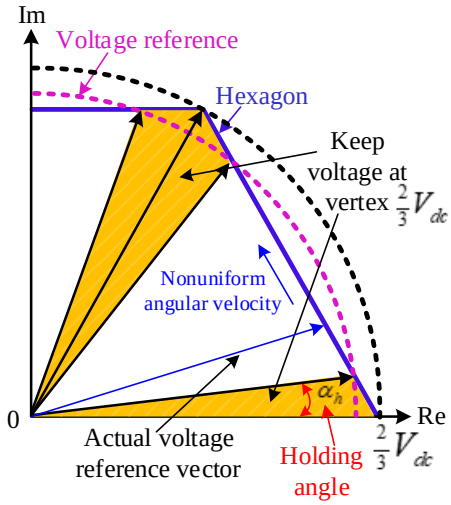

Figure 4. Voltage reference trajectory in overmodulation mode II (zone II).

3. DISTORTED CURRENTS IN OVERMODULATION OPERATION

The harmonic components of the output voltage appear in the OVM range, in which the components of the even-order and triplen harmonics are naturally removed in three-phase systems. Thus, the presence of the 5th, 7th, 11th, 13th order harmonics and so on should be considered in the output voltage of PWM inverter. The output voltage space vector (u^s) in the stationary reference frame is expressed as [1, 4]

$$u^s = u_1(e^{j\omega_e t} + K_5 e^{-j5\omega_e t} + K_7 e^{j7\omega_e t} + K_{11} e^{-j11\omega_e t} + K_{13} e^{j13\omega_e t} + \cdots) \quad (2)$$

where u_1 is the fundamental output voltage component and K_j (j = 5, 7, 11, 13, …) is the ratio of n^{th} harmonic component and its fundamental.

When the inverter output voltage is fed to the machine, then the harmonic currents in the machine caused by the harmonic voltage components are expressed as

$$i^s = i_1(e^{j\omega_e t} + K_{i5} e^{-j5\omega_e t} + K_{i7} e^{j7\omega_e t} + K_{i11} e^{-j11\omega_e t} + K_{i13} e^{j13\omega_e t} + \cdots) \quad (3)$$

where i^s is the machine current vector in the stationary reference frame, i_1 is the fundamental current component, and K_{ij} (j = 5, 7, 11, 13, …) is the ratio of n^{th} harmonic current components to its fundamental value.

For vector-controlled machine drives, the machine current controller implemented in the rotating reference frame, in which the machine current vector (i^e) is expressed as

$$\begin{aligned} i^e &= i^s \cdot e^{-j\omega_e t} \\ &= i_1(1 + K_{i5} e^{-j6\omega_e t} + K_{i7} e^{j6\omega_e t} + K_{i11} e^{-j12\omega_e t} + K_{i13} e^{j12\omega_e t} + \cdots) \end{aligned} \quad (4)$$

Equation (4) presents the DC quantity and multi-sixth order harmonic current components of the machine. Figure 5 shows the fast Fourier transform (FFT) analysis of the machine current and the inverter output voltage. As can be seen from the figure, the fundamental and fifth- and seventh-order components of stator and currents exist in the stationary reference frame and the DC component and the multi-sixth order harmonics of the stator current appear in the synchronous reference frame.

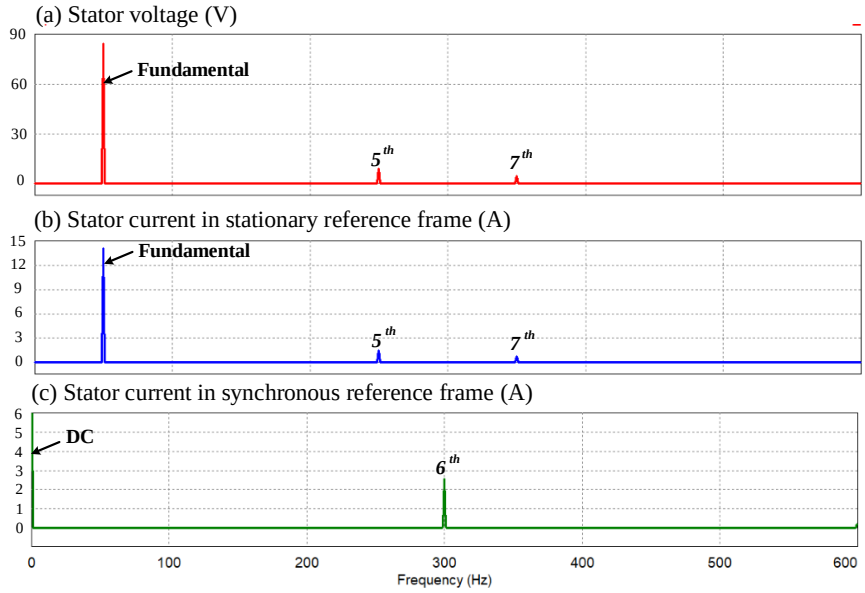

Figure 5. FFT analysis of stator voltage and current waveforms.

4. MODELING AND CONTROL OF INDUCTION MOTOR

4.1. Modeling of induction motor

The *dq*-axis voltage equations in stationary reference frame are written as [10, 11]

$$\begin{cases} V_{ds}^{s} = R_s i_{ds}^{s} + \dfrac{d}{dt}\lambda_{ds}^{s} \\ V_{qs}^{s} = R_s i_{qs}^{s} + \dfrac{d}{dt}\lambda_{qs}^{s} \\ 0 = R_r i_{dr}^{s} + \dfrac{d}{dt}\lambda_{dr}^{s} + \omega_r \lambda_{qr}^{s} \\ 0 = R_r i_{qr}^{s} + \dfrac{d}{dt}\lambda_{qr}^{s} + \omega_r \lambda_{dr}^{s} \end{cases} \quad (5)$$

where V_{ds}^{s}, V_{qs}^{s}, i_{ds}^{s}, and i_{qs}^{s} are the *dq*-axis stator voltage and current, respectively, R_s, R_r are the stator and rotor resistances, respectively, ω_r is the rotor speed, λ_{ds}^{s}, λ_{qs}^{s}, λ_{dr}^{s}, and λ_{qr}^{s} are the *dq*-axis stator and rotor fluxes, respectively. The stator and rotor fluxes are expressed as

$$\begin{cases} \lambda_{ds}^{s} = L_s i_{ds}^{s} + L_m i_{dr}^{s} \\ \lambda_{qs}^{s} = L_s i_{qs}^{s} + L_m i_{qr}^{s} \\ \lambda_{dr}^{s} = L_r i_{dr}^{s} + L_m i_{ds}^{s} \\ \lambda_{qr}^{s} = L_r i_{qr}^{s} + L_m i_{qs}^{s} \end{cases} \quad (6)$$

where L_s=L_{ls}+L_m, L_r=L_{lr}+L_m in which L_{ls} and L_{lr} are the stator and rotor leakage inductance, L_m is the magnetizing inductance, i_{dr}^{s} and i_{qr}^{s} are the *dq*-axis rotor current components, respectively.

From the rotor flux linkage and the stator current, the machine torque (T_e) is expressed as

$$T_e = \frac{3P}{4}\frac{L_m}{L_r}\left(\lambda_{dr}^s i_{qs}^s - \lambda_{qr}^s i_{ds}^s\right) \qquad (7)$$

where P is the number of poles.

4.2. Motor control

By applying the rotor flux-oriented control ($\lambda_{qr} = 0$), the rotor flux linkage exists on the d-axis only. Hence, the magnitude of the rotor flux ($\lambda_{r,mag}$) is expressed as

$$\lambda_{r,mag} = \lambda_{dr} = L_m I_{ds} \qquad (8)$$

where λ_{dr} , λ_{qr} and I_{ds} are the dq-axis components of the rotor flux and stator current expressed in synchronous rotating reference frame.

The machine torque is rewritten as

$$T_e = \frac{3P}{4}\frac{L_m}{L_r}\lambda_{dr} I_{qs} \qquad (9)$$

where I_{qs} is the q-axis stator current in synchronous dq reference frame.

From (8) and (9), the rotor flux linkage and the machine torque can be adjusted by controlling the d-axis stator current and the q-axis stator current, respectively.

As shown Figure 5, the feed-forward terms (V_{ds}^{ff} , V_{qs}^{ff}) in synchronous reference frame for the decoupling control can be expressed as

$$\begin{aligned} V_{ds}^{ff} &= -\omega_e \sigma L_s I_{qs}^* \\ V_{qs}^{ff} &= \omega_e L_s I_{ds}^* \end{aligned} \qquad (10)$$

where ω_e is the synchronous angular frequency and $\sigma = 1 - \frac{L_m^2}{L_s L_r}$ is the leakage factor.

In the OVM range, the PI controller can not work well since the multi-sixth order harmonics are included in the machine currents which affect the performance of the control system considerably. To achieve the fast torque control of the vector-controlled drives, a large bandwidth of the current controller is required. In this case, the harmonic components in the feedback current will damage the performance of the PI current controller.

To improve the performance of the current controller in OVM ranges, the multi-sixth order harmonics of the current in the synchronous reference frame needs to be removed. To do this, a band-pass filter is applied to extract only DC component in the measured current before it is fed to the current controller. The reference voltages obtained from the output of the current controllers are pre-processed by the static OVM strategy. Thus, the modified reference voltages are produced by the PWM inverter. As for the current controller, the controller gains (k_p, k_i) must be properly designed in OVM range to reduce the overshoot of the current controller response at the corner of the hexagon. Hence, the k_p and k_i are selected as

$$\begin{aligned} k_p &= L_{tr}\frac{\omega_{cc}}{2} \\ k_i &= R_{tr}\frac{\omega_{cc}}{2} \end{aligned} \qquad (11)$$

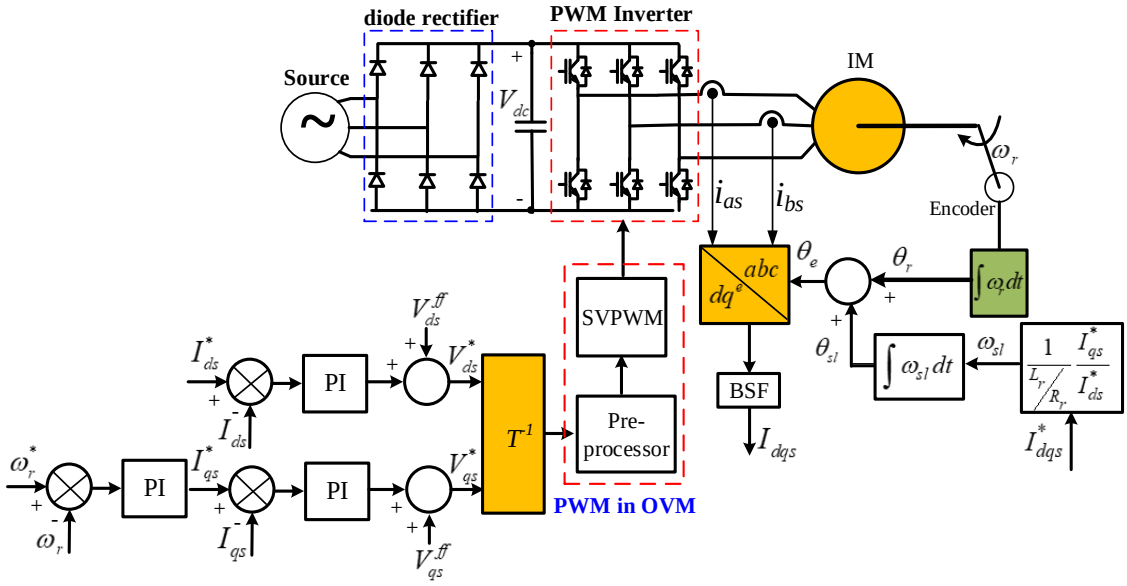

Figure 6. Block diagram of vector-controlled IM drives.

where R_{tr} and L_{tr} are the equivalent stator resistance and transient stator inductance, respectively. ω_{cc} is the cut-off frequency. Figure 6 shows the block diagram of the vector-controlled induction motor drives.

5. SIMULATION RESULTS

PSIM simulation has been carried out for a 3 kW-induction machine drive model under full-load condition to verify the effectiveness of the proposed method. The parameters of the induction motor are listed in the Table 1. The inverter input voltage is 331V, provided by a front-end diode rectifier to produce OVM operation modes. The switching frequency is 5 kHz.

Table 1. Parameters of induction motor

Parameter	Value
Rated power	3 kW
Stator voltage/frequency	220 V_{rms}/50 Hz
Stator resistance	0.533 Ω
Rotor resistance	0.93 Ω
Stator/rotor inductance	3 mH
Magnetizing inductance	76 mH
Number of poles	4
Generator inertia	0.0033 kg.m^2

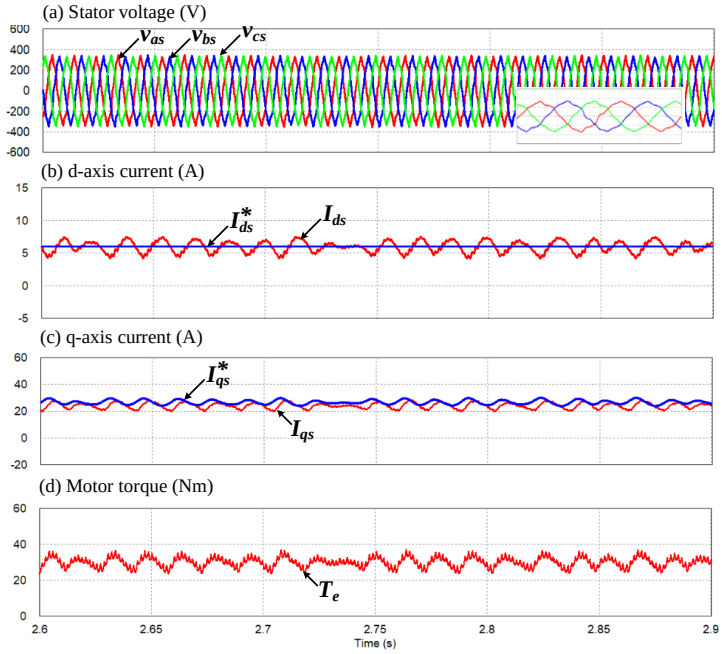

Figure 7. Performance of current controllers without harmonic current elimination (m = 0.95).

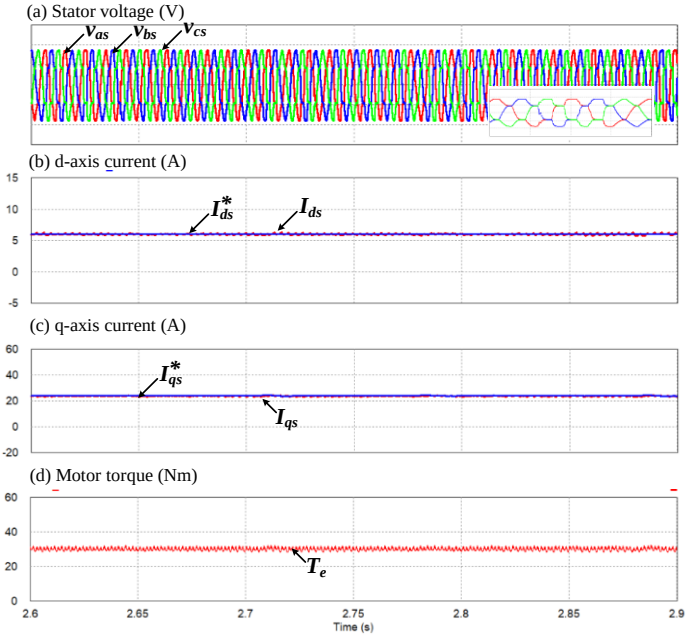

Figure 8. Performance of current controllers with harmonic current elimination (m = 0.95).

Figure 7 and 8 show the comparison of the current control performances between the two methods: the conventional method (without harmonic current elimination) and the proposed one (with harmonic current elimination) under the full load condition, in which the modulation index of the inverter is 0.95 at the operating speed of 2810 rpm. The current controllers with harmonic compensation give better performance than those without harmonic compensation. As can be clearly seen in Figure 8(b) and (c), the *dq*-axis currents in the proposed method have lower ripples than those in the conventional one (see Figure 7(b) and (c)). Also, the motor torque ripple (see Figure 8(d)) in the proposed method is significantly reduced, compared with torque in the conventional one, as shown in Figure 7(d). With the conventional method, the

total harmonic distortion (THD) factors of the stator voltage in phase A, phase B and phase C in Figure 7(a), which are calculated thanks to the available THD function on Simview of PSIM software, are 23.905%, 27.502% and 30.833%, respectively. Meanwhile, with the proposed method, the THD factors of the stator voltage in phase A, phase B and phase C are 8.125%, 9.877% and 10.205%, respectively. By comparison, the stator voltage in the proposed method is less distorted than that in the conventional one since the THD factors in the proposed method are about three times smaller than those in comparison with the conventional one.

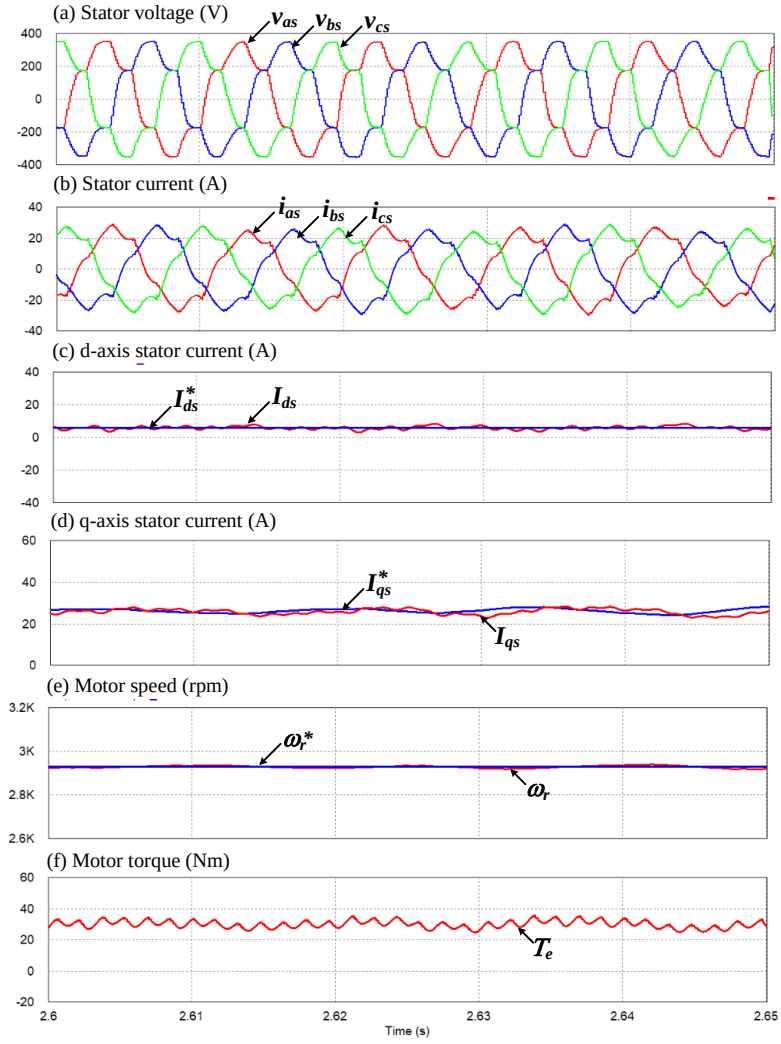

Figure 9. Performance of the motor under overmodulation range (m = 0.986).

By applying the proposed method, the performance of the machine under OVM range (m = 0.986) of the PWM inverter is shown in Figure 9. Due to the presence of harmonic components in the stator voltage, as shown in Figure 9(a), the dq-axis stator currents in Figure 9(b) and (c) are much distorted. Despite this, the operation of the machine can be kept stable. During this operation mode, the measured machine speed follows its reference well, in which the percentage of the speed error is less than 1%, as shown in Figure 9(d). Figure 9(e) shows the machine torque, of which distortion is around 25%.

Figure 10 shows the performance of the machine in transient state, in which the machine speed reference is changed from 2810 rpm at 2 s to 2940 rpm at 2.05 s. The machine still operates stably. In this condition, the operation mode of the PWM inverter is changed from

the OVM mode I (m = 0.95) to mode II (m = 0.989). It is observed in Figure 10(b) that the machine currents in OVM mode I are less distorted than those in OVM mode II. The q-axis machine current in Figure 10(d) is much increased at the moment of speed reference change. As shown in Figure 10(e), the machine speed is controlled to follow its reference well and the machine speed in OVM mode II are much more oscillated than that in OVM mode II. The machine torque is increased fast to accelerate the machine speed to its command, as shown in Figure 10(f).

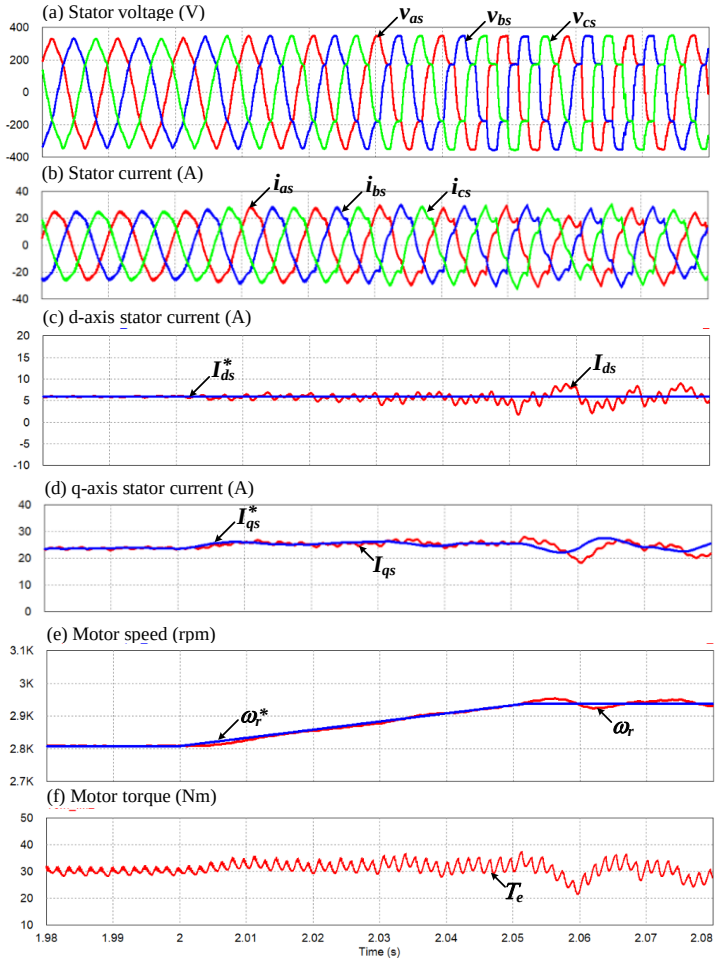

Figure 10. Performance of the motor in transient state.

6. CONCLUSION

In this research, a control performance of vector-controlled induction motor drives has been investigated in overmodulation range, in which the multi-sixth order harmonic components can be removed from the feedback current. For this, the PI current controller gives good performance regardless of the existence of the harmonic currents. Also, the speed and torque ripples of the machine are much mitigated. The proposed method is more effective for the maximum utilization of the machine torque. The validity of the proposed method is verified by the PSIM simulation results.

Acknowledgements: This work was funded by Ho Chi Minh City University of Food Industry (Contract number 52 HD/DCT dated September 3, 2019).

REFERENCES

1. Lee D. C. and Lee G. M. - A novel overmodulation technique for space-vector PWM inverters, IEEE Transactions Power Electronics **13** (6) (1998) 1144-1151.
2. Holtz J., Lotzkat W., and Khambadkon A. - On continuous control of PWM inverters in the overmodulation range including the six-step mode, IEEE Transactions on Power Electronics **8** (4) (1993) 546-553.
3. Bolognani S. and Zigliotto M. - Novel digital continuous control of SVM inverters in the ovemodulation range, IEEE Transactions on Industry Applications **33** (2) (1997) 525-530.
4. Khambadkone A. M., Holtz J. -Compensated synchronous PI current controller in overmodulation range and six-step operation of space-vector modulation-based vector controlled drives, IEEE Transactions on Industrial Electronics **49** (3) (2002) 574-579.
5. Venugopal S. and Narayanan G. - An overmodulation scheme for vector controlled induction motor drives, 2006 International Conference on Power Electronic, Drives and Energy System (2006) 1-6.
6. Tripathi A., Khambadkone A. M., Sanjib K. Panda - Stator flux based space-vector modulation and closed loop control of the stator flux vector in overmodulation into six-step mode, IEEE Transactions on Power Electronics **19** (3) (2004) 775-782.
7. Tripathi A., Khambadkone A. M., Sanjib K. Panda - Direct method of overmodulation with integrated closed loop stator flux vector control, IEEE Transactions on Power Electronics **20** (5) (2005) 1161-1168.
8. Tripathi A., Khambadkone A.M., Sanjib K. Panda - Dynamic control of torque in overmodulation and in the field weakening region, IEEE Transactions on Power Electronics **21** (4) (2006) 1091-1098.
9. Modi M.K., Venugopal S., Narayanan G. - Space vector-based analysis of overmodulation in triangle-comparison based PWM for voltage source inverter, Indian Academy of Sciences **38** (2013) 331-358.
10. Sul S. K. - Control of electric machine drive systems, New Jersey: Wiley (2011).
11. Bose B. K. - Power electronics and AC drives. New Jersey: Prentice-Hall (1987).

TÓM TẮT

ĐIỀU KHIỂN ĐỘNG CƠ KHÔNG ĐỒNG BỘ TRONG VÙNG QUÁ ĐIỀU CHẾ

Văn Tấn Lượng*, Đoàn Xuân Nam, Lê Thành Tới
Trường Đại học Công nghiệp Thực phẩm TP.HCM
*Email: *luongvt@hufi.edu.vn*

Bài báo đề xuất một chiến lược điều khiển của động cơ không đồng bộ (IM) trong phạm vi quá điều chế (OVM) để cực đại việc sử dụng điện áp của bộ nghịch lưu nguồn áp (VSI). Trong vùng quá điều chế, việc điều chế độ rộng xung vector không gian (SVPWM) được tạo ra bởi điện áp tham chiếu bổ sung, từ đó có thể làm cho dòng điện động cơ bị méo dạng, dẫn đến phá hủy vận hành điều khiển bộ VSI. Để cải thiện vận hành điều khiển hệ thống, các thành phần họa tần dòng điện cần được loại bỏ trước khi đưa vào bộ điều khiển dòng điện dùng bộ tích phân-tỷ lệ (PI). Sự đáp ứng của bộ điều khiển dòng điện trong phạm vi quá điều chế được phân tích và cho vận hành tốt. Phương pháp đề xuất được xác minh bằng kết quả mô phỏng động cơ không đồng bộ công suất 3kW.

Từ khóa: Máy điện không đồng bộ, quá điều chế, điều khiển vector.